

Micro actuated grating for multi-beam optical pickups

Chi-Hung Lee

Department of Photonics & Institute of Electro-optical Engineering National Chiao Tung University, Hsin-Chu 300, Taiwan, R. O. C.

E-mail: tainanncku@hotmail.com

Yi Chiu

Department of Electrical and Control Engineering National Chiao Tung University, Hsin-Chu 300, Taiwan, R. O. C.

E-mail: yichiu@mail.nctu.edu.tw

Han-Ping D. Shieh

Department of Photonics & Display Institute National Chiao Tung University, Hsin-Chu 300, Taiwan, R. O. C.

Abstract: A stress-induced curved polysilicon actuator with a grating is achieved for the application of recordable optical pickups, which have been realized on a single silicon chip using a two-layer poly-silicon and one-layer silicon nitride micro-machining process. Three diffracted beams with equal intensity in each order from the grating were generated while applying a voltage to the actuator. The switching between the single beam and multiple beams can be applied for writing data and reading data in the disc, respectively.

©2007 Optical Society of America

OCIS codes: (050.1950) Diffraction gratings; (210.0210) Optical data storage; (220.4000) Microstructure fabrication; (350.3950) Micro-optics.

References and links

1. A. Alon and J. Finkelstein, World Patent WO 98/37554 (1998).
2. A. Alon and T. Kosoburd, "Multi-beam optical pickup," U.S. Patent. No. 6,411,573 (2002).
3. R. Katayama, K. Yoshihara, Y. Yamanaka, M. Tsunekane, K. Kayanuma, T. Iwanaga, O. Okada, and Y. Ono, "Multi-beam optical disk drive for high data transfer rate systems," *Jpn. J. Appl. Phys., Part 1* **31**-2B, 630-634 (1992).
4. H. Okumura, K. Arai, N. Kawamura, H. Tokumaru, and H. Okuda, "Multi-beam light source using optical waveguide for optical recording," *Proc. SPIE* **4090**, 329-334 (2000).
5. Hsi-Fu Shih, "Multiple-beam liquid crystal grating for the recordable optical pickup head," *Jpn. J. Appl. Phys.*, **44**, 1815-1817 (2005).
6. W.-H. Lee, "High efficiency multiple gratings," *Appl. Opt.* **18**, 2152-2158 (1979).
7. E. K. Chan and R. W. Dutton, "Effects of capacitors, resistors and residual charge on the static and dynamic performance of electrostatically-actuated devices," *Proc. SPIE* **3680**, 120-130 (1999).
8. M. A. Rosa, D. D. Bruyker, A. R. Volkkel, E. Peeters, and J. Dunec, "A novel external electrode configuration for the electrostatic actuation of MEMS based devices," *J. Micromech. Microeng.* **14**, 446-451(2004).
9. J C Chiou and Y J Lin, "A novel large displacement electrostatic actuator: pre-stress comb-drive actuator," *J. Micromech. Microeng.* **15**, 1641-1648 (2005).
10. F. P. Beer and E. R. Johnston, *Mechanics of Materials*. 2nd Ed., (McGraw-Hill, NY, 1992)

1. Introduction

Increasing the data rate in optical storage system has been attracting much attention, particularly for high quality TV programs which require a data-transfer rate of more than 100 Mbps. In conventional CD and DVD drives, an optical pickup (OPU) with a single laser beam

for sequential data retrieving is used. The data rate is proportional to the rotation speed of the spindle motor. However, the maximum rotation speed is confined by the frequency response characteristics of the objective lens actuator. Using multi-beam in parallel is a straightforward solution to increase the data rate. Several methods have been demonstrated to achieve simultaneous reading on multiple tracks. Depending on the methods of generating multiple beams, at least three types have so far been reported: a diffractive optical element [1-2], a diode laser array [3], and a combination of laser diodes and a beam combiner [4]. In 1998, Alon et al. proposed a pickup using the diffractive optical element method [1]. A grating was used to split an illumination beam into a plurality of reading beams with equal intensities, which were then projected onto a plurality of tracks of the optical storage medium. Multiple beams can be generated uniformly by the grating, the development of a recordable multi-beam OPU is limited due to insufficient power in each beam. To overcome the limitation, Shih et al. proposed a multi-beam liquid crystal grating, which can alternatively switch between single-beam recording and multi-beam retrieving [5].

In this paper, we presented a silicon-based free-space dynamic grating, which is composed of a binary phase micro-grating and a bimorph actuator, to enable the switching between single-beam recording and multi-beam retrieving. Low stress silicon nitride as the optical material is used for its high transparency in the visible spectrum, and superior chemical and mechanical properties. The low-voltage electrostatically bimorph actuator is achieved using a stress-induced curved polysilicon.

2. Optical design and simulation

The free-space integrated micro-optical pickup is based on the surface micromachining technology. Optical components such as elliptical diffractive lenses, folded mirrors, polarization beam splitter and the dynamic grating are integrated on an optical bench. The dynamic grating consists of a vertical binary phase grating that can be raised above the path of the incident beam for data recording [Fig. 1(a)] and lowered to create multiple beams for data retrieving [Fig. 1(b)]. The substrate serves as a free-space optical bench for the integrated optical system.

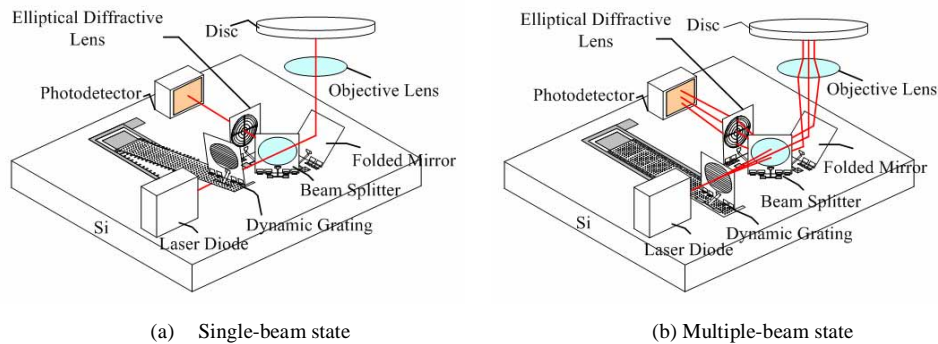


Fig. 1. Schematic of the dynamic grating based micro-optical pickup by stress-induced bending of polysilicon cantilever beam. States for (a) the single-beam recording and (b) the multiple-beam retrieving.

2.1 Binary phase micro-grating

Assuming the number of beams is three, the optical spots are formed using a three-beam grating. To read data on the disc, the 0th order beam intensity I_0 should be equal to the ± 1 st order beam intensities $I_{\pm 1}$. The diffraction angle is determined by the optical system layout such as the working distance, the thickness of the cover layer of the disc, and the spacing between the 0th order beam and the ± 1 st order beams on the disc, as shown in Fig. 2.

To determine the diffraction angle of the first-order beams, the current design assumed

40- μm spot pitch on the disc. Because the spot pitch is wider than track pitch, the spot array would be positioned at an angle from radial direction in practical application. For a 100- μm thick cover layer with refractive index of 1.6, the equivalent air thickness of the cover layer is 62.5 μm . If the working distance between the objective lens and the cover layer is 460 μm , under the thin lens approximation for the objective lens, the diffraction angle, θ , is about 4.35°. For a transmissive grating with $\theta=4.35^\circ$, $m=1$ and $\lambda=632.8$ nm, the period Λ is about 8.35 μm , derived from the equation $\Lambda \times \sin\theta = m \times \lambda$. $\Lambda=8$ μm was selected in the design. To reduce the process complexity, a grating with rectangular shape was designed using the commercial software G-Solver.

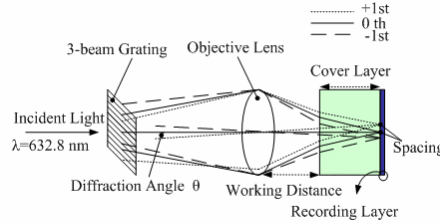


Fig. 2. Optical path of the three beams for tracking.

The diffraction energy distribution, I_0 and I_1 , of a grating can be determined by the period, the line-width and the depth of the grating, denoted by Λ , w , and D , respectively, as follows [6];

$$I_o = [(2f - 1) \sin \theta]^2 + \cos^2 \theta \quad (1)$$

$$I_1 = \left[2 \left(\frac{\sin m\pi f}{m\pi} \right) \sin \theta \right]^2$$

where $m=1$ is the diffracted order and $f=w/\Lambda$, is defined as the ratio of the line-width to the grating period, and is related to the depth of the grating D and the refractive index n of grating material, low stress silicon nitride, by the formula

$$\frac{D(n-1)}{\lambda} = \frac{\theta}{180} \quad (2)$$

where $n=2.102+0.008i$ at $\lambda=632.8$ nm.

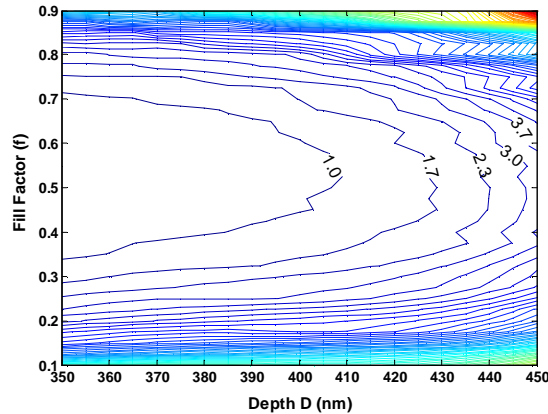


Fig. 3. Diffraction ratio ($I_0/I_{\pm 1}$) contours for various values of the fill factor f and of the grating depth D .

It is found when the fill factor is 0.50, multiple grating depths may be selected. For example, at 176 nm, 404nm, 756nm and 972 nm, the intensities of the three beam are equal. Other grating depths meeting the requirement are higher than 1000 nm, which is not suitable in surface micromachining processes. To have sufficient mechanical strength and reasonable fabrication yield, the depth of 404 nm was selected. The contour plot of the diffraction ratio $I_0/I_{\pm 1}$ is shown in Fig. 3 for several values of D and f . A diffraction ratio ($I_0/I_{\pm 1}$) of about 1 is obtained provided that $f=0.5$ and $D=404\text{nm}$.

2.2 Bimorph actuator

To switch between the state of single beam and the state of multiple beams, the actuation distance in the free end of the bimorph actuator requires to be larger than $400\ \mu\text{m}$. In a standard electrostatic ‘parallel plate’ system, the actuation is controlled by an electrode parallel to and directly underneath an actuated element. The motion is determined by the balance between the electrostatic force and the mechanical restoring force. For a linear restoring force, the actuation distance is only one third of its actuation range [7]. To overcome the limit of small actuation distance, Rosa *et al.* proposed an external electrode bi-morph actuator, which allows the operation of electrostatic actuators to be controlled over their entire range of motion by preventing electrostatic pull-in instability [8]. However, the fringe effect between the moving and fixed external electrodes is relatively insufficient to obtain enough actuating force.

Accordingly, the bimorph actuator we use is based on the concept of Chiou *et al.*, which used comb-shape external electrodes and post heat treatment to achieve higher actuation distance under lower voltages [9]. If σ_1 and σ_2 are the material stress, and E_1 and E_2 are the Young’s moduli of material 1 (polysilicon) and 2 (Cr-Au), respectively, the height z of the free end of the actuator can be described by the curvature ρ of the bimorph actuator as follows [10];

$$\rho = \frac{Eh(3m + \frac{K}{n(1+n)^2})}{6(\sigma_2 - m\sigma_1)} \dots\dots\dots (3)$$

$$K = 1 + 4mn + 6mn^2 + 4mn^3 + m^2n^4$$

$$z = \rho(1 - \text{Cos} \frac{L}{\rho})$$

where, $E=E_1$, $m=E_1/E_2$, $n=n_1/n_2$, and L is the length of the bimorph actuator.

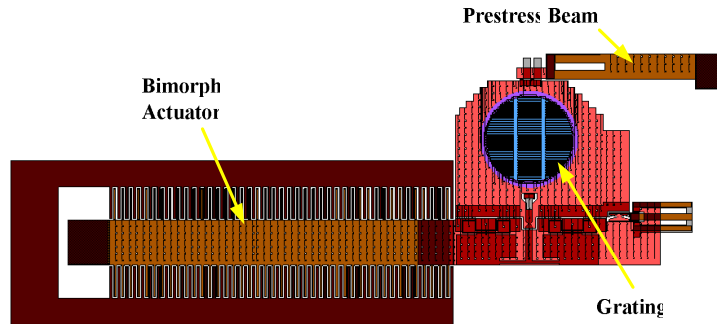


Fig. 4. The layout of the proposed dynamic grating, which consists of a bi-morph actuator, on which a grating is mounted. The pre-stress beam is used to assist lifting the released grating during the assembling.

As illustrated in Fig. 4, the proposed dynamic grating consists of a $2000 \times 260 \mu\text{m}^2$ bimorph beam fixed to a bonding pad, with a binary phase grating attached to the other end using microhinges and microspring latches. 43 movable comb-shape fingers are orthogonally mounted on each side of the composite beam, while 86 fixed comb fingers are mounted on the surface of the nitride isolation layer. Here the engaged length of the comb finger is designed to be $180 \mu\text{m}$ in average. The two arrays of fixed combs beside the movable comb are connected to another bonding pad for driving signals. A stress layer of Cr-Au is deposited on the polysilicon layer to curve upwards the beam after process releasing, because the Cr-Au is under tensile residual stress while the polysilicon is under compressive residual stress. To actuate the switch, a voltage is applied to create the fringe effect between the fixed combs and the moving combs.

To fabricate the device, an isolation layer of $0.6 \mu\text{m}$ thick silicon nitride (SiN) was first deposited. After growing a $2\text{-}\mu\text{m}$ -thick sacrificial silicon dioxide (SiO_2), $0.7\text{-}\mu\text{m}$ -deep dimples and $2\text{-}\mu\text{m}$ -deep anchors were then patterned in the sacrificial layer shown in Fig. 5(a). The first structural poly-Si and optical layer SiN_x were then deposited and patterned to form a micro-frame shown in Fig. 5(b). The thickness of SiN_x layers would be further reduced to the target value at the HF releasing step. After growing a $2\text{-}\mu\text{m}$ -thick SiO_2 and patterning anchors, the second structural poly-Si layer was deposited and patterned to implement the micro-spring latches and the first layer of cantilever beam. The wafer was annealed for two hours at 1050°C in nitrogen to reduce the residual film stress. A 140-nm -thick Cr film and a $0.5\text{-}\mu\text{m}$ -thick Au film were deposited on the cantilever to induce the internal stresses shown in Fig. 5(c). Upon releasing in hydrofluoric (HF) vapor at 40°C , the cantilever beam curved upward to lift the micrograting off the substrate. A micro-probe was then used to assemble the micrograting to vertical position.

The SEM micrograph of a dynamic grating with a central aperture of $500 \mu\text{m}$ in diameter is shown in Fig. 6(a). Using the same process, the dynamic grating was integrated with other components to form other optical elements shown in Fig. 6(b).

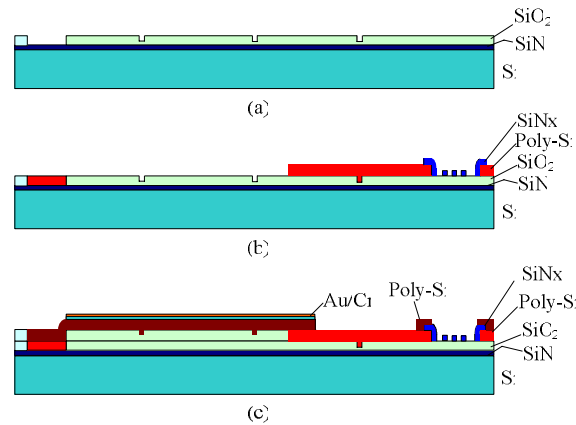


Fig. 5. Process flow for the dynamic grating. (a) The first dimple-etch and anchor-etch after the first silicon dioxide deposition. (b) Low stress silicon nitride patterning after the first poly-silicon deposition and patterning. (c) The Cr/Au films and the second poly-silicon deposition and patterning after the second silicon dioxide deposition and the second anchor-etch.

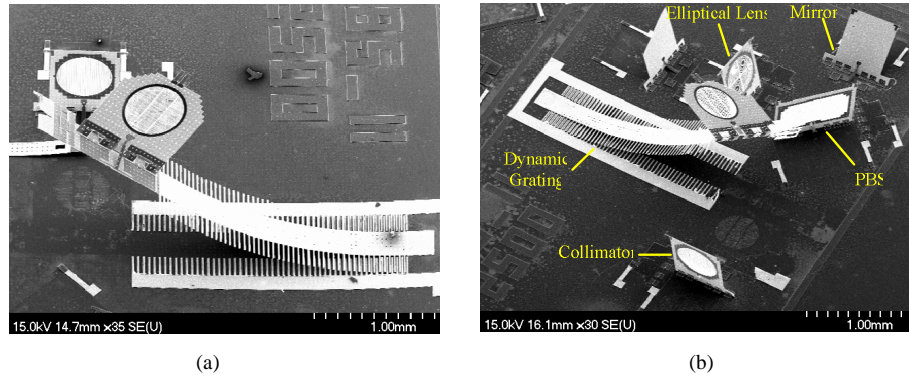


Fig. 6. SEM of a (a) dynamic grating and (b) micro optical elements in a optical pickup.

3. Experimental results and discussion

The static characteristics of the bimorph actuator with a grating were obtained by applying a dc bias driving voltage at the fixed comb fingers. The measured lift height of the free end versus the applied dc bias driving voltage is shown in Fig. 7. A typical nonlinear characteristic over the entire actuation range, 1200 μm between 0 and 80 V, is observed.

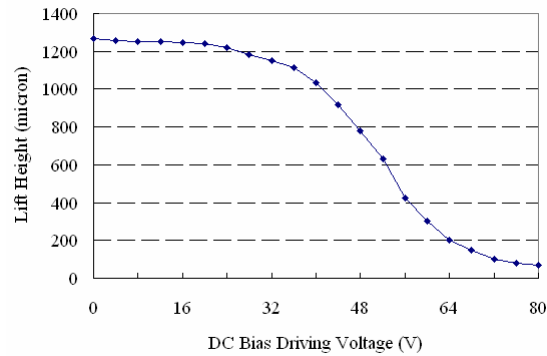


Fig. 7. Static lift heights of the free end versus dc bias driving voltages.

To measure the optical performance of the micro devices, a He-Ne laser at $\lambda=632.8\text{nm}$ was used as the light source. To block the noise from outside of the optical pattern area, an aperture of a diameter 350 μm was used to yield the incident beam size, which is smaller than the grating area of a diameter 500 μm . The beam alignment tolerance is 75 μm in the measurement. A polarizer was adjusted to obtain the required polarization states. The optical patterns were measured by a CCD camera positioned at 10 mm from the dynamic grating.

As shown in Fig. 8 (a), no voltage was applied to have the incident beam propagate directly for recording use. As shown in Fig. 8(b), an external voltage of 80 volts was applied to have the incident beam pass through the binary phase grating for reading use. For the micro-grating, the measured Gaussian beam widths of the -1st, 0th, and +1st order beams were 271 μm , 293 μm , and 278 μm , respectively, which means the diffraction intensity distribution is symmetric. The measured diffraction angle at far field was 4.51 $^\circ$, which agrees well with the theoretical value of 4.53 $^\circ$. The normalized measured diffraction intensities of the -1st order beam, 0th order beam and the +1st order beam are 0.93, 1 and 0.91, respectively. There was 57.1% of the incident power distributed among the three useful orders whereas the calculated efficiency was 67.6%. The deviation from the target value of 1 for each beam was mainly due to the thickness variation, index variation, dimples, the roughness of the sidewall and the surface of the grating. The mean roughness was 5.3 nm in average, which introduced

phase variation and affected the energy distribution of the diffracted beams.

The thickness variation and roughness of the silicon nitride film as influenced by film growth and HF releasing can cause phase differences and scattering of the light at the interface. Besides, the thermal stress between the silicon nitride film and the poly-silicon plate distorted the intensity profile of the main beam.



Fig. 8. Diffraction patterns (a) before and (b) after applying voltage to the actuator.

4. Conclusion

Using a two-layer poly-silicon and one-layer low stress silicon nitride surface micromachining process, a dynamic micro-grating composed of a binary phase grating and a bimorph actuator was demonstrated. The optical pattern area of the grating is $500\ \mu\text{m}$ in diameter. The voltage required to switch the grating is 80 volts. The measured diffraction angle is 4.51° . The normalized measured diffraction intensities of the -1st order beam, 0th order beam and the +1st order beam are 0.93, 1 and 0.91. The optical performance of the dynamic grating shows its potential for integration with other micro-optical elements for multibeam optical pickups application.

Acknowledgments

This work is supported by the Ministry of Economic Affairs under grant number 93-EC-17-A-S1-0011.